THE ASTROPHYSICAL JOURNAL, 407:L29–L32, 1993 April 10

NEAR-INFRARED OBSERVATIONS OF THE HH 111 REGION

ROLAND GREDEL AND BO REIPURTH
European Southern Observatory, Casilla 19001, Santiago 19, Chile;
e-mail: rgredel@eso.org; reipurth@eso.org
Received 1992 December 11; accepted 1993 January 25

ABSTRACT

We have obtained near-infrared *K*-band images of the HH 111 region, and detected, besides the HH 111 jet itself, a new optically invisible bipolar jet here called HH 121, from the source region of HH 111, but at large angles to the HH 111 flow axis. Near-infrared long-slit spectra of both jets confirm their emission-line nature. Radial velocities derived from H_2 lines show that the northern lobe of HH 121 is approaching and the southern is receding, but the velocities are so low that the system is likely to lie almost in the plane of the sky. There is a considerable angle between the two lobes of HH 121. The HH 111 and HH 121 jets intersect within an arcsecond of a VLA source, and we interpret the observations as two bipolar jets emanating from a putative pre–main-sequence binary, a situation very similar to the HH 1/2 region. Tidal forces could effect significant precession and disturbance of the disk around the lower mass stellar component, possibly causing the large discrepancy between the flow axes of HH 111 and HH 121 and between the lobes of HH 121 itself. Near-infrared [Fe II] lines have been used to derive electron densities ($n_e \approx 2000$ cm^{-3}) and extinction ($A_V \approx$ 5–6 mag) in parts of the HH 111 jet, and H_2 lines were employed to derive an excitation temperature of about 2150 K.

Subject headings: ISM: individual (HH 111) — ISM: jets and outflows — stars: formation — stars: pre–main-sequence

1. INTRODUCTION

The HH 111 jet is one of the best-collimated jets known to emanate from a young star. The HH complex consists of a jet, a faint counterjet, and several bow shocks on either side of an embedded 25 $L_\odot$ *IRAS* source. The total extent of the complex is 367″, which at the assumed distance of 460 pc corresponds to 0.82 pc in projection. The HH complex is inclined 10° to the plane of the sky, with the western lobe approaching and the eastern lobe receding along the line of sight, and with space velocities directed away from the infrared source of up to 600 km s^{-1} (Reipurth 1989; Reipurth, Raga, & Heathcote 1992).

Recently, the driving source was detected at the VLA, and was found to be displaced 5″ from a near-infrared source, suggesting that this source is a nearby IR reflection nebula (Rodríguez & Reipurth 1993). The dense structure observed by Stapelfeldt & Scoville (1993) with the Owens Valley interferometer is also centered on the position of the VLA source.

In this *Letter* we present deep near-infrared images and long-slit spectra of the HH 111 jet region. We show that a second faint bipolar jet, HH 121, emanates from the source at a large angle to the HH 111 jet, strongly suggesting that the source is a binary system. We use near-infrared long-slit spectra to infer H_2 excitation conditions and to determine the extinction and the electron density in the HH 111 jet.

2. OBSERVATIONS

The *K*-band image presented here was obtained on 1992 October 12/13 with the ESO 2.2 m telescope at La Silla, using the Infrared Array Camera (IRAC2) with a 256 × 256 pixel HdCdTe detector. The final frame is an average of 120 exposures with a detector integration time (DIT) of 10 s each. Explicit sky observations were carried out in 3 minute intervals, and difference images of a halogen lamp with the lamp on and off were used as flat fields. Long-slit spectroscopy of the HH 111 jet was performed on 1992 September 10/11 and October 10/11 under photometric conditions. The data were collected with the Infrared Spectrometer (IRSPEC) on the ESO 3.5 m New Technology Telescope (NTT). A 58 × 62 pixel InSb detector was used, with a pixel scale of 2.″2 on the sky. The entrance slit width was set to 2 pixels, corresponding to a spectral resolution $R = \lambda/\Delta\lambda \approx 2500$. The slit was aligned along the HH 111 jet using a position angle (P.A.) of 97° and centered on knot H by offsetting from reference star 8, using the coordinates given by Reipurth (1989) and Reipurth & Olberg (1991). The grating was set to various lines of H_2 and [Fe II]; total integration times were 5–25 minutes with DITs of 40–60 s. The H_2 (1, 0) *S*(1) line was observed toward the HH 121 jet on 1992 November 6/7 under nonphotometric conditions. Two exposures were obtained of 5 × 60 s each, with the slit centered on knots B (P.A. = 36°) and Y (P.A. = 34°).

3. NEAR-INFRARED OBSERVATIONS OF HH 111/HH 121

Figure 1 shows a contour plot of our *K*-band image of the HH 111 region. The HH 111 jet shows up prominently, and the knots H, L, and P, in the notation of Reipurth (1989), are identified. The shift reported between the infrared source (IRS) and the VLA source (Rodríguez & Reipurth 1993) is confirmed. The infrared source is clearly extended and diffuse. The major surprise, however, is the presence of a set of knots, A, B, C, located on a line through the VLA source but inclined by 119°, in projection, to the axis of the HH 111 jet. South of IRS there is another set of fainter knots, X, Y, Z, forming an angle of ≈80° to the HH 111 axis. The long-slit spectra show that the new knots are emitters in H_2, and are not reflected light or background stars. We here denote this new shocked outflow HH 121. The observed properties of the knots in HH 121 are summarized in Table 1. Positions were derived relative to the positions of knots H and P in the HH 111 jet as given in

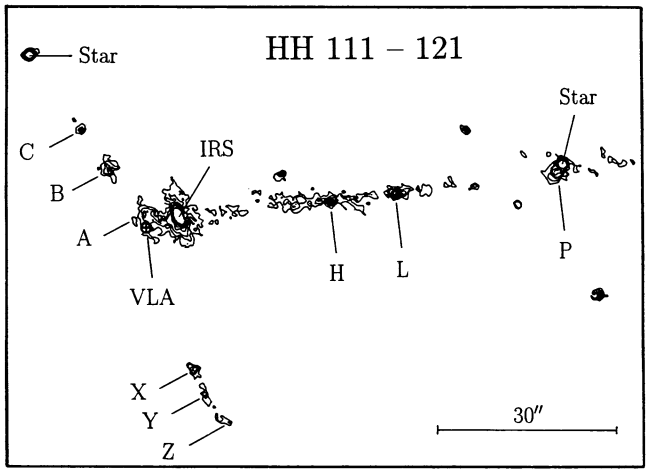

FIG. 1.—Contour plot of the *K*-band image of the HH 111–HH 121 complex.

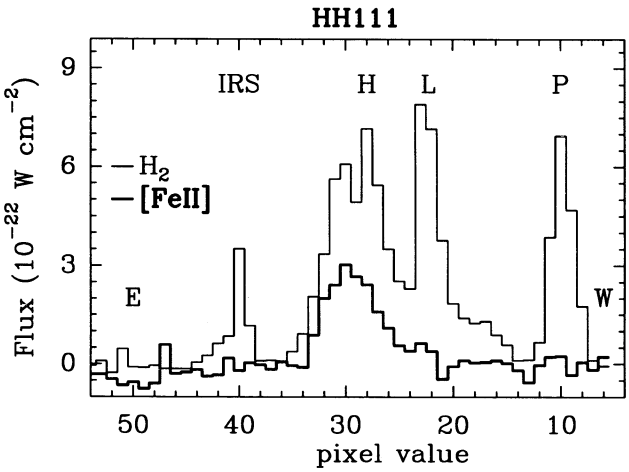

FIG. 2.—Flux in the H_2 2.121 μm and in the [Fe II] 1.644 μm line along the HH 111 axis. The spatial scale is 2.″2 pixel^{-1}. The [Fe II] intensity is scaled by a factor of 0.2.

Reipurth (1989). We estimate the resulting accuracy to be of the order of 1″–2″.

Figure 2 shows the variation of the intensity in the H_2 (1, 0) $S(1)$ line along the HH 111 jet. Local maxima in H_2 occur near knots H and P, which have very low excitation ([S II]/H$\alpha \approx$ 2–3), and near knot L, which is of high excitation ([S II]/H$\alpha \approx$ 0.5) (Morse 1992). Also shown in Figure 2 is the spatial distribution of the [Fe II] $a^4D_{7/2}$–$a^4F_{9/2}$ line, scaled by a factor of 0.2. Local maxima in [Fe II] occur near those in [S II], which, in the HH 111 jet, are regions of high electron densities n_e (Morse 1992). [Fe II] is not detected if n_e drops below 1000 cm^{-3}, which is also found in HH 91 (Gredel, Reipurth, & Heathcote 1992).

Table 2 summarizes the H_2 and [Fe II] observations in HH 111. For H_2 the line designation, the transition wavelength in air, the excitation energy $E(v'J')$ of the upper level $(v'J')$, and the integrated line fluxes for knots H, L, P, and IRS as measured in 7, 2, 4, and 4 pixel apertures, respectively, are given. For [Fe II], the excitation energies above the [Fe II] $a^6D_{9/2}$ level are given in column (2). Line fluxes are listed for knots H and L (12 pixel aperture) and IRS (4 pixel aperture).

The [Fe II] lines measured allow us to infer n_e and the extinction toward the HH 111 jet. The ratio between the [Fe II] $a^4D_{1/2}$–$a^4F_{5/2}$ and the $a^4D_{7/2}$–$a^4F_{9/2}$ lines is sensitive to n_e (see, e.g., Oliva, Moorwood, & Danziger 1990). Using their diagram (their Fig. 7), our measured value of 0.03 in knot H would indicate n_e around 2000 cm^{-3}, with an error margin of $10^3 < n_e < 10^4$ cm^{-3}. The value is in agreement with $n_e \approx$ 1000 cm^{-3} (Reipurth 1989) and n_e = 2000–5000 cm^{-3} (Morse 1992), inferred from [S II]. Toward IRS we get $n_e \approx 10^4$–10^5 cm^{-3}, which is close to the critical density for collisional de-excitation of the [Fe II] 1.644 μm line (Kawara, Nishida, & Taniguchi 1988). The reddening can be determined from the [Fe II] $a^4D_{7/2}$–$a^4F_{9/2}$ and $a^4D_{7/2}$–$a^6D_{9/2}$ lines, which arise from a common upper level. Adopting the Einstein A-values of Nussbaumer & Storey (1988) a value of $E_{J-H} \approx 0.06$ mag is inferred, corresponding to A_V = 5–6 mag (Draine 1989). Toward IRS we get $E_{J-H} \geq 1$ mag, or $A_V \geq 10$ mag. We use these values to correct the H_2 fluxes for extinction. The H_2 data are analyzed as reiterated by, e.g., Gredel et al. (1992). Figure 3 contains the excitation diagram for knots H, L, P, and IRS, where ln $N(v'J')/g$ is plotted against $E(v'J')$. $N(v'J')$ are the population densities inferred for levels $(v'J')$, and g are the statistical weights. Filled and open symbols represent data with and without extinction corrections, respectively. The H_2 population distribution in all three knots H, L, and P is consis-

TABLE 1

OBSERVATIONS OF KNOTS IN HH 121

KNOT	POSITION α(1950)	POSITION δ(1950)	H_2 FLUX[a] (10^{-22} W cm^{-2})
A	5^{h}49^{m}09^s.2	+2°47′50″	4
B	5 49 09.7	+2 47 58	11
C	5 49 10.0	+2 48 04	6
X	5 49 08.7	+2 47 24	12
Y	5 49 08.5	+2 47 19	9
Z	5 49 08.3	+2 47 15	4

[a] (1, 0) $S(1)$ line, 50% uncertainty.

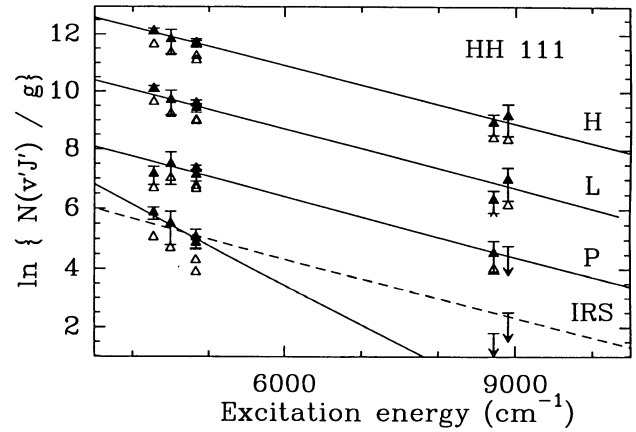

FIG. 3.—H_2 excitation diagrams for HH 111 knots H, L, P, and IRS. Filled and open symbols represent data with and without extinction corrections, respectively. The ordinate is valid for knot H only. The ln $N(v'J')/g$ data points are shifted by −1.3, −3.6, and −5.0 units for knots L, P, and IRS, respectively. The straight line for knots H, L, and P and the dashed line for IRS indicate T_{ex} = 2150 K; the straight line for IRS is T_{ex} = 950 K.

TABLE 2

LINE INTENSITIES IN THE HH 111 JET

LINE	λ_{air} (μm)	$E(v'J')$ (cm^{-1})	$I(v'J')$[a] (10^{-22} W cm^{-2}) Knot H	Knot L	Knot P	IRS
H_2 Lines						
(1, 0) $S(7)$	1.748	8908	6.5 (3.2)	2.4 (1.2)	≤ 3	≤ 0.7
(1, 0) $S(1)$	2.121	4831	36.0 (3.6)	15.0 (1.5)	17.4 (1.7)	3.9 (0.8)
(2, 1) $S(1)$	2.247	8723	3.3 (1.2)	0.8 (0.3)	1.5 (0.7)	≤ 0.3
(1, 0) $Q(1)$	2.406	4274	29.0 (2.9)	13.0 (1.3)	7.5 (2.2)	5.9 (1.2)
(1, 0) $Q(2)$	2.413	4498	8.5 (3.4)	3.4 (1.4)	4.1 (2.0)	1.6 (0.8)
(1, 0) $Q(3)$	2.423	4831	29.0 (4.3)	10.0 (1.5)	11.0 (2.2)	4.1 (1.2)
[Fe II] Lines						
$a^4D_{7/2}$–$a^6D_{9/2}$	1.257	7955	87 (15)	...		≤ 6
$a^4D_{7/2}$–$a^4F_{9/2}$	1.644	7955	113 (12)	...		11 (2)
$a^4D_{1/2}$–$a^4F_{5/2}$	1.664	8847	3.4 (1)	...		1.7 (1)

[a] Uncertainties in parentheses.

tent with a thermal excitation of $T_{ex} = 2150 \pm 400$ K, indicated by the straight lines. The excitation temperature in IRS appears lower, $T_{ex} \approx 950$ K, but the inferred H_2 fluxes may be affected by inaccurate continuum subtraction.

Radial velocities can be determined from the near-infrared lines to an accuracy of about 20 km s^{-1} through measurements relative to telluric OH emission lines that appear in the raw frames. Using the OH wavelengths and line identifications of Oliva & Origlia (1992), we infer heliocentric velocities of $V_\odot \approx -40$ km s^{-1} for knots H, L, and P in HH 111, and in HH 121 $V_\odot \approx +10$ km s^{-1} for knots A, B, and C and $V_\odot \approx +30$ km s^{-1} for knots X, Y, and Z. The [Fe II] line toward knot H appears near $V_\odot \approx -60$ km s^{-1}, in excellent agreement with the velocity of [S II] of $V_\odot = -63$ km s^{-1} (Reipurth 1989). The heliocentric velocity of the cloud is +23 km s^{-1}. Knots A, B, and C thus lie in a slightly blueshifted lobe and knots X, Y, and Z in a slightly redshifted lobe.

4. DISCUSSION

Inspection of very deep optical CCD images through red broad- and narrow-band filters reveals no trace of the HH 121 knots. This is perhaps not surprising, since they are located in a part of the cloud core with very high extinction, as judged from the complete absence of visual background stars. The fact that the knots emit in H_2 suggests that they are shocks, and combined with their alignment on an axis passing through the central VLA/*IRAS* source, the inescapable conclusion is that HH 121 is a second bipolar jet, emanating from the source region of the HH 111 complex.

If the source is a binary, the explanation of a double jet is straightforward. The double jet in the HH 1/2 complex, which is very similar to the present case except that both jets are optically visible, indeed has a double VLA source (Reipurth et al. 1993a). Double or multiple jets are also known from looser aggregates of young stars, such as the HL Tau region and the HH 24 region (Mundt, Ray, & Bührke 1988; Mundt, Ray, & Raga 1991). Finally, we note that binaries among pre–main-sequence stars are ubiquitous (e.g., Reipurth & Zinnecker 1993). We thus conclude that a binary central source is the most likely explanation for the double jets we observe.

The two axes of the main lobes of HH 111 and HH 121 cross each other at a point less than 1″ from the VLA source, which is approximately the accuracy with which the optical and radio coordinate systems are connected in this part of the sky (Rodríguez et al. 1990). It thus would seem that we have an upper limit of about 500 AU for the projected separation between the two binary components. The binary system is surrounded by a substantial amount of cold gas and dust; the large 1300 μm flux toward the VLA source of 490 mJy translates into a circumbinary mass of between 0.5 and 3.3 $M_\odot$, depending on the choice of mass absorption coefficient (Reipurth et al. 1993b). Part of this considerable mass is likely to be in a large infalling envelope, but almost certainly an important fraction would be in circumstellar disks closely surrounding the individual binary components. One possible way to understand the flow geometry we observe is to assume that the jets are ejected perpendicular to the circumstellar disks. Tidal forces will induce precession of the disks, in particular of the less massive disk.

There is a rather major angle, about 15°–20°, between the axes of the two lobes of HH 121. Differences between the flow axes are common in HH flows, although this angle is exceptionally large. There is a well-determined difference of 1° between the two lobes of the HH 111 system. Theoretical models of disks around binary stars show that substantial warping can take place (Terquem & Bertout, private communication), and we speculate that the difference in angle between the lobes is induced by differences in the "upper" and "lower" sides of the individual disks. If so, the much larger angle between the HH 121 lobes compared with the HH 111 lobes might suggest that the driving source of the HH 111 jet is the more massive of the two stars, and that the source of HH 121 is a lower mass companion star.

It has been argued that HH flows are intermittent phenomena related to disk accretion events, possibly of the FU Orionis type (e.g., Reipurth 1989). A T Tauri disk can be perturbed by a close encounter with a binary companion star in a highly eccentric orbit in such a way that the accretion rate through the disk increases by a factor of 100 or 1000, an event we would observe as a FUor outburst (Clarke, Lin, & Pringle 1990). The fact that two jets are generated simultaneously by the companions in our putative binary may suggest that they result from a common perturbation.

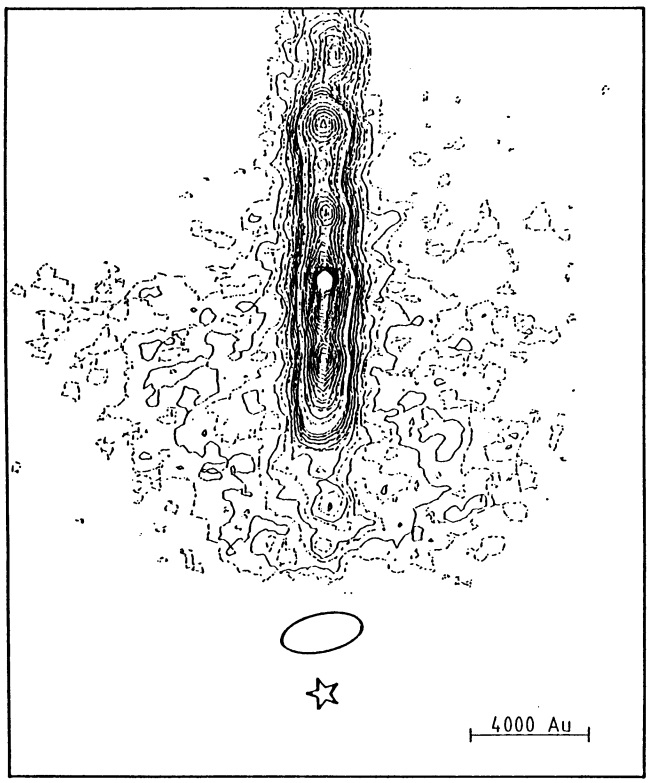

FIG. 4.—Illustration of the HH 111 region based on optical, infrared, and radio data. The contour plot of the jet and V-shaped reflection nebula is based on a [S II] CCD image, the ellipse indicates the infrared reflection nebula, and the asterisk is at the position of the VLA source.

The IRS, formerly thought to be the embedded driving source, is clearly an extended reflection nebula. It consists of a centrally brightened ellipsoid, with the major axis at an angle of $\approx 75°$ in projection to the jet axis. The dimensions of the ellipse at a level of 1/10 of the central flux are approximately $3'' \times 6''$, which at a distance of 460 pc correspond to 1400×2800 AU. A better understanding of this region comes from Figure 4, which shows a mosaic of optical, infrared, and radio data. The upper part is a [S II] CCD image from Reipurth (1989), the ellipsoid is a stylized presentation of the infrared reflection nebulosity, and the asterisk shows the VLA position from Rodríguez & Reipurth (1993). The large V-shaped nebula is light reflected toward us from the embedded source. The angle of the jet to the plane of the sky is only 8°, so the star is probably embedded in a disk seen almost edge-on (Reipurth et al. 1992). In the optical, light is scattered in a cone about 15,000 AU high and 15,000 AU at its widest. The base of the reflection nebula can only be seen in the infrared. The elongated IR reflection nebula is presumably the illuminated sides of the cavity which the outflowing jet has evacuated in the disk and envelope. The source itself is occulted by the almost edge-on disk and is only observed in radio emission.

Recently, Whitney & Hartmann (1992, 1993) have calculated images of light scattered in flared disks and in dusty envelopes around young embedded stars. The dimensions and appearances of these calculations show a remarkable correspondence to what we observe. This supports an interpretation of the optical and infrared reflection nebulae as due to light scattered in a large infalling envelope, the accretion of which ultimately drives the highly collimated jet.

REFERENCES

Clarke, C. J., Lin, D. N. C., & Pringle, J. E. 1990, MNRAS, 242, 439
Draine, B. T. 1989, in Proc. 22d ESLAB Symp. On Infrared Spectroscopy in Astronomy (ESA SP-290; Paris: ESA), 93
Gredel, R., Reipurth, B., & Heathcote, S. 1992, A&A, 266, 439
Kawara, K., Nishida, M., & Taniguchi, Y. 1988, ApJ, 328, L41
Morse, J. A. 1992, Ph.D. thesis, Univ. North Carolina
Mundt, R., Ray, T. P., & Bührke, T. 1988, ApJ, 333, L69
Mundt, R., Ray, T. P., & Raga, A. C. 1991, A&A, 252, 740
Nussbaumer, H., & Storey, P. J. 1988, A&A. 193, 327
Oliva, E., Moorwood, A. F. M., & Danziger, I. J. 1990, A&A, 240, 543
Oliva, E., & Origlia, L. 1992, A&A, 254, 466
Reipurth, B. 1989, Nature, 340, 42
Reipurth, B., Chini, R., Krügel, E., Kreysa, E., & Sievers, A. 1993b, A&A, in press
Reipurth, B., Heathcote, S., Roth, M., Noriega-Crespo, A., & Raga, A. C. 1993a, ApJ, in press
Reipurth, B., & Olberg, M. 1991, A&A, 246, 535
Reipurth, B., Raga, A. C., & Heathcote, S. 1992, ApJ, 392, 145
Reipurth, B., & Zinnecker, H. 1993, A&A, in press
Rodríguez, L. F., Ho, P. T. P., Torrelles, J. M., Curiel, S., & Cantó, J. 1990, ApJ, 352, 645
Rodríguez, L. F., & Reipurth, B. 1993, in preparation
Stapelfeldt, K. R., & Scoville, N. Z. 1993, ApJ, in press
Whitney, B. A., & Hartmann, L. 1992, ApJ, 395, 529
———. 1993, ApJ, 402, 605